A Biophysical Model of Atrial Fibrillation to Simulate the Maze III Ablation Pattern

C Tobón, C Ruiz, JF Rodríguez, F Hornero, JM Ferrero (Jr.), J Sáiz

I3BH, Universidad Politécnica de Valencia, Spain

Abstract

Atrial fibrillation (AF) is the most common cardiac arrhythmia. The Maze III ablation pattern consists of creating lines of conduction block in both atria to prevent multiple wavelets. In this work we simulated the Maze III pattern in a tridimensional (3D) model of human remodeling atria and evaluated its efficacy for termination of an AF episode. To carry out the study, an episode of AF was generated by ectopic activity in the left pulmonary veins. Unipolar pseudo-electrograms were computed. When we applied the Maze III ablation pattern, the AF was finished after 200 ms. The developed model can be implemented to improve ablation patterns in order to find an ideal pattern to allow ending the arrhythmia with the least number of lines of ablation.

1. Introduction

Atrial fibrillation (AF) is the most common cardiac arrhythmia. Typically atrial tachycardias are characterized by rapid activation of the atria (300-500 bpm) [1]. This rapid activation causes atrial remodelling; it provokes a set of changes in atrial properties that induces electrical changes [2-4]. These electrical changes cause a decrease in refractoriness due to a significant action potential duration (APD) shortening [3;4]. This is expected to allow the initiation and the maintenance of reentrant waves in the atrial tissue [2;5].

Several treatments are available to restore sinus rhythm: medication, electrical cardioversion, atrial pacing, surgical and catheter ablation [6;7]. The objective of ablation is to create lines of conduction block to prevent formation and maintenance of multiple wavelets. The surgical Maze ablation was proposed by Cox *et al.* [8]. This procedure consists of applying surgical incisions to both atria according to a specific pattern. Although a high success rate was reported (80–99%), the results were difficult to reproduce and many clinical complications were observed [9]. More recently, percutaneous radiofrequency (RF) catheter ablation was proposed as a less invasive alternative to surgical ablation. On the basis of the Maze operation different series of lesion patterns were suggested [8-10] An ideal pattern should be able to prevent AF with a limited number of ablation lines of minimal length, while allowing for maintenance or recovery of mechanical activity of both atria during sinus rhythm. However, this ideal ablation pattern is still unknown.

The evaluation of different lesion patterns is usually performed in clinical studies or in animal experiments. The main drawbacks of animal experiments lie in the difficulty to technically access the whole atria and in the differences between animal and human anatomy.

Advanced computer technology allows develop sophisticated biophysical models, which allow the simulation of the mechanisms involved in AF and opens up innovative approaches to simulate potential treatments.

In this work we simulated the Maze III pattern in a tridimensional model of human atria and evaluated its efficacy for termination of an AF episode.

2. Method

2.1. 3D model of human atria

A computer model of the human atria developed in previous work [11] was used. The model includes the main anatomical structures: left and right atrial chambers (LA and RA), inter-atrial septum, pectinate muscles (PMs), limbus of the fossa ovalis, Bachmann's bundle (BB), crista terminalis (CT), left and right appendages (APG), coronary sinus (CS), right and left pulmonary veins (RPV and LPV), superior and inferior caval veins (SCV and ICV), isthmus of right atrium and openings corresponding to the valves (see figure 1). An area near superior caval vein was defined as the sinoatrial node.

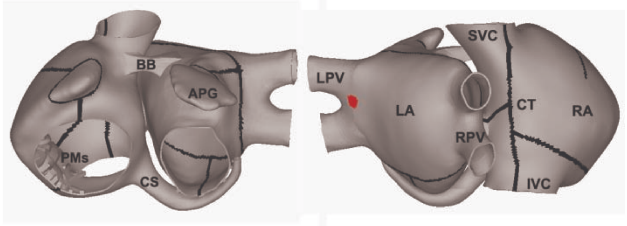

Figure 1. 3D model of human atria, including the ablation

lines of the Maze III procedure. The red dot is the ectopic focus.

The atrial surface is discretized into a hexahedral mesh with 52906 elements and 100554 nodes. The model has a realistic fiber orientation.

In this work, the electrophysiological heterogeneity was included to reproduce measured action potentials [12]. For this, maximum conductances of I_t, I_{Kr} and I_{CaL} were modified in the Nygren's cellular model for CT, PMs, atrial APG and atrioventricular rings. Anisotropic conduction was assumed. The transversal to longitudinal ratio of conductivity for CT was 1:9, for the atrial working myocardium (AWM) was 1:2 and the isthmus and the SAN were set to be isotropic. The conduction velocity were 69 cm/s for AWM, 120 cm/s for BB and PMs, 143 cm/s for CT, 54 cm/s for PVs, 44 cm/s for isthmus and 25 cm/s for SAN.

2.2. Electrical remodeling

Experimental data reported by Bosh *et al.* [3] have demonstrated that atrial fibrillation induces changes in ionic channel conductance and kinetics of human atrial myocytes. These changes have been incorporated in the model of human atrial action potential (AP) developed by Nygren *et al.* [13] to reproduce atrial remodeling. In order to get the remodeling model, several parameters were changed in the AP model: the channel conductance for I_{K1} was increased by 250%, the channel conductance for I_{CaL} was decreased by 74%, the channel conductance for I_t was decreased by 85%, the kinetics of the fast inactivation of I_{CaL} was increased by 62%, the activation curve of I_t was shifted by +16 mV and the inactivation curve of I_{Na} was shifted by +1.6 mV. These values are taken from data published by Zhang *et al.* [14]. With these changes, the modified model can reproduce the action potential of human atrial myocytes of patients with permanent AF. This modified electrophysiological model was integrated in the 3D model.

2.3. Action potential propagation

Action potential propagation was modeled using the monodomain equation given by:

$$\nabla \cdot Di \nabla V_m = S_v \left(C_m \frac{dV_m}{dt} + I_{ion} \right) \quad (1)$$

where V_m is the transmembrane potential, C_m = 50 pF/cm2 is the specific membrane capacitance, S_v is the cell surface-to-volume ratio, D_i is the conductivity tensor, and I_{ion} is the aggregate ion fluxes. The ion fluxes across the membrane are based on the modified Nygren atrial cellular model. Extracellular space with infinite resistance is assumed. Equation 1 was solved using a finite element method.

2.4. Ablation pattern Maze III

Linear transmural lesions caused by surgical ablation procedures are modelled by selecting elements of the model, which were assigned zero conductivity in order to become real obstacles to the activation fronts (black lines in figure 1).

2.5. Pseudo-electrograms

Pseudo unipolar electrograms (EGMs) were computed in 43345 simulated-electrodes located on the model surface. The extracellular potential (Φ_e) was modelled using a current source approximation for a large volume conductor:

$$\Phi_e(r,t) = \frac{1}{4\pi\sigma_e} \int dr' \frac{I_m(r',t)}{|r-r'|} \quad (2)$$

where r is the electrode location vector, r' is the current source location vector, I_m is the transmembrane current per unit area of atrial tissue surface, and σ_e is the extracellular conductivity. EGMs were computed every millisecond. This electrograms was then used to calculate the power spectral density using Fast Fourier Transform (FFT) method, which allowed us to obtain the maximum dominant frequency (DF).

2.6. Stimulation protocol

AF was generated by S1-S2 protocol. A train of stimuli was applied during 10 seconds in the sinoatrial node area to simulate the sinus rhythm. The basic cycle length (BCL) was 1000 ms. After, an ectopic beat was applied near to left pulmonary veins at a tight coupled interval (red dot in figure 1).

The ablation lines of the Maze III procedure were applied after 10 seconds of AF.

3. Results and discussion

The electrical remodeling induced a 7 mV hyperpolarization of the resting potential, a 70% reduction in APD_{90} (90% repolarization) and 5% reduction in conduction velocity. The APD_{90} was reduced from 284 ms to 86 ms. These changes are consistent with experimental observations [3;4].

The ectopic focus generated reentrant activity leading to fibrillatory conduction. The ectopic beat applied near to left PVs during the repolarization phase of the tenth sinus beat, generated a unidirectional block. The wavefront turned around the PVs and it continued propagating generating reentrant waves. This result is accord with experimental studies [15-18]. Observations published by Hobbs *et al.* [15], demonstrated the role of electrical remodelling in the progression of focal atrial

ectopy to AF. Others studies published by Haissaguerre *et al.* [16], Chen *et al.* [17], and Kumagai *et al.* [18], shows the role of focal activation in the initiation and maintenance of AF, initiated by triggers in the pulmonary veins (PV's); which could be successfully treated by delivery of radiofrequency energy (RF).

The width of the vulnerable window for reentry (range of time in which reentries occur) was 16 ms.

Figure-of-eight reentries, rotors and collisions were observed during 10 seconds of simulation (see figure 2). Figure-of-eight reentries have been observed experimentally [19] and in simulations of cardiac tissue [20]. Equally, experimental and computational studies [21-24], have been obtained rotors in the atrium.

The pseudo-electrograms obtained show variability in size and shape during simulated AF. Electrogram complexes were rapid, irregular and polymorphous (variability in size and shape). Irregularity and polymorphism was greater during figure-of-eight reentry and collisions, during rotor activity the electrograms shown more uniform and regular complexes. Spectral analysis of the electrograms shows broadbands with multiple frequency peaks, as a consequence of the unstable electrical activity. FFT analysis has had increasing use in helping to study and characterize atrial arrhythmias [23;25]. The Figure 2 shows an example of pseudo-electrogram calculated in the center of left free wall.

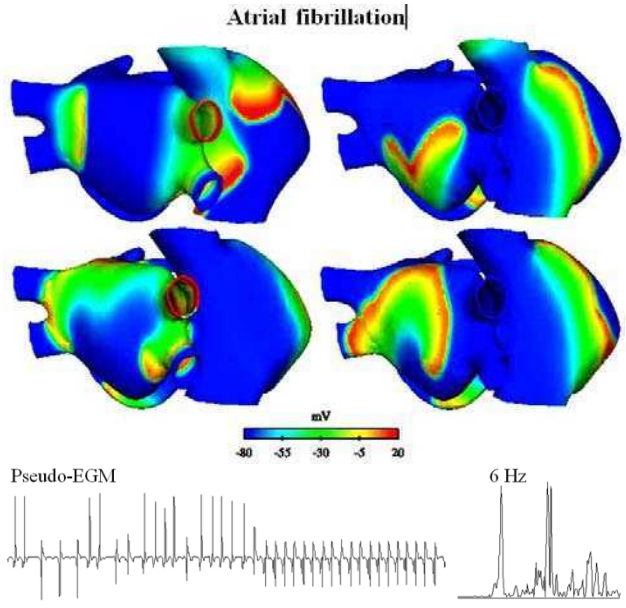

Figure 2. AF triggered by ectopic activity. The red colour represents the despolarization voltage and blue colour the repolarization voltage. Under the figures shows an example of pseudo-electrogram calculated in the center of left free wall and it spectral analyse.

When we applied the Maze III ablation pattern, the AF was finished after 200 ms. The ablation lines in the right atrium blocked the wave fronts in this area. Similarly, ablation lines in the left atrium prevented that the reentrant fronts on the left free wall continue their activity. The front of depolarization ended in the right PVs and superior caval vein (see figure 3).

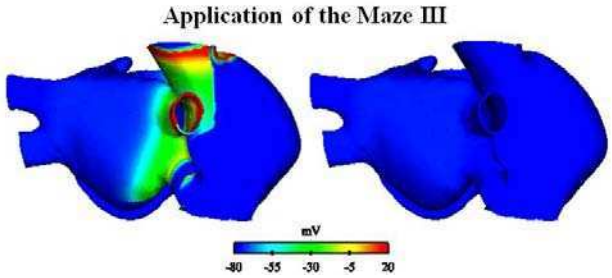

Figure 3. Maze III procedure terminated the AF.

4. Conclusions

The results have been consistent with several cases reported by clinical studies. The developed model can be implemented to improve ablation patterns in order to find an ideal pattern to allow ending the arrhythmia with the least number of lines of ablation.

Acknowledgements

This work was partially supported by the "Plan Nacional de Investigación Científica, Desarrollo e Innovación Tecnológica del Ministerio de Educación y Ciencia" of Spain (TEC 2005-04199 and TEC 2008-02090).

References

[1] Nattel S. New ideas about atrial fibrillation 50 years on. Nature 2002;415(6868):219-26.

[2] Wijffels MCEF, Kirchhof CJHJ, Dorland R, Allessie MA. Atrial-fibrillation begets atrial-fibrillation - a study in awake chronically instrumented goats. Circulation 1995;92(7):1954-68.

[3] Bosch RF, Zeng X, Grammer JB, Popovic CM, Kuhlkamp V. Ionic mechanisms of electrical remodelling in human atrial fibrillation. Cardiovasc. Res. 1999;44:121-31.

[4] Workman AJ, Kane AK, Rankin AC. The contribution of ionic currents to changes in refractoriness of human atrial myocytes associated with chronic atrial fibrillation. Cardiovasc. Res. 2001;52(2):226-35.

[5] Veenhuyzen GD, Simpson CS, Abdollah H. Atrial fibrillation. Canadian Medical Association Journal 2004;171(7):755-60.

[6] Ninio DM. Contemporary management of atrial fibrillation. Aust. Prescr. 2000;23:100–102,.

[7] Petrac D. Electrical therapy of atrial fibrillation. J. Clin. Basic Cardiol. 2001;4:123–129.

[8] Cox JL, Schuessler RB, D'Agostino HJ (Jr), Stone CM,

Chang BC, Cain ME, Corr PB, and Boineau JP. The surgical treatment of atrial fibrillation: III. Development of a definitive surgical procedure. J. Thorac. Cardiovasc. Surg. 1991;101:569–583.

[9] Sie HT, Beukema WP, Elvan A and Misier AR. Newstrategies in the surgical treatment of atrial fibrillation. Cardiovasc. Res. 2003;58:501–509.

[10] Sueda T, Nagata H, Shikata H, Orihashi K, Morita S, Sueshiro M, Okada K and Matsuura Y. Simple left atrial procedure for chronic atrial fibrillation associated with mitral valve disease. Ann.Thorac.Surg. 1996;62(6):1796-1800.

[11] Ruiz-Villa C, Tobón C, Rodríguez JF, Ferrero JM, Hornero F and Saíz J. Influence of atrial dilatation in the generation of re-entries caused by ectopic activity in the left atrium. Computers in Cardiology 2009;36:457−460.

[12] Feng J, Yue L, Wang Z and Nattel S. Ionic mechanisms of regional action potential heterogeneity in the canine right atrium. Circ.Res. 1998;83(5):541-551.

[13] Nygren A, Fiset C, Firek L, Clark JW, Lindblad DS, Clark RB and Giles WR. Mathematical model of an adult human atrial cell: the role of K+ currents in repolarization. Circ. Res. 1998;82(1):63-81.

[14] Zhang H, Liu J-H, Garratt CJ and Holden AV. Cellular modelling of electrical remodelling in two different models of human atrial myocytes. Computers in Cardiology 2003;30:777-80.

[15] Hobbs WJ, Van Gelder IC, Fitzpatrick AP, Crijns HJ, Garratt CJ. The role of atrial electrical remodelling in the progression of focal atrial ectopy to persistent atrial fibrillation. Journal of Cardiovascular Electrophysiology 1999;10:866-70.

[16] Haïssaguerre M, Jais P, Shah DC, Takahashi A, Hocini M, Quiniou G. Spontaneous initiation of atrial fibrillation by ectopic beats originating in the pulmonary veins. N. Engl. J. Med. 1998;339:659-66.

[17] Chen SA, Hsieh MH, Tai CT, Tsai CF, Prakash VS, Yu WC. Initiation of atrial fibrillation by ectopic beats originating from the pulmonary veins. Electrophysiological characteristics, pharmacological responses, and effects of radiofrequency ablation. Circulation 1999;100:1879-86.

[18] Kumagai K, Yasuda T, Tojo H, Noguchi H, Matsumoto N, Nakashima H et al. Role of rapid focal activation in the maintenance of atrial fibrillation originating from the pulmonary veins. Pace-Pacing and Clinical Electrophysiol 2000;23(11):1823-7.

[19] Uno K, Kumagai K, Khrestian CM, Waldo AL. New insights regarding the atrial flutter reentrant circuit: Studies in the canine sterile pericarditis model. Circulation 1999;100:1354-60.

[20] Vigmond EJ, Tsoi V, Kuo S, Arevalo H, Kneller J, Nattel S, Trayanova N. The effect of vagally induced dispersion of action potential duration on atrial arrhythmogenesis. Heart Rhythm 2004;3:334-44.

[21] Jalife J. Rotors and spiral waves in atrial fibrillation. J. Cardiovasc. Electrophysiol 2003;14:776-80.

[22] Skanes AC, Mandapati R, Berenfeld O, Davidenko JM and Jalife J. Spatiotemporal periodicity during atrial fibrillation in the isolated sheep heart. Circulation 1998;98:1236-48.

[23] Mandapati R, Skanes AC, Chen J, Berenfeld O, Jalife J. Stable microreentrant sources as a mechanism of atrial fibrillation in the isolated sheep heart. Circulation 2000;101:194-9.

[24] Wieser L, Nowak CN, Tilg B and Fischer G. Mother rotor anchoring in branching tissue with heterogeneous membrane properties. Biomed.Tech.(Berl) 2008;53(1):25-35.

[25] Ryu K, Sahadevan J, Khrestian CM, Stambler BS, Waldo AL. Use of fast fourier transform analysis of atrial electrograms for rapid characterization of atrial activation-implications for delineating possible mechanisms of atrial tachyarrhythmias. J. Cardiovasc. Electrophysiol. 2006; 17:198-206.

Address for correspondence.

Catalina Tobón Zuluaga
Instituto Interuniversitario de Investigación en Bioingeniería
y Tecnología Orientada al Ser Humano (UPV)
Ciudad Politécnica de la Innovación - Cubo Azul - Edif. 8B - Acceso N
Camino de Vera s/n, 46022 - Valencia (Spain)
E-mail: ctobon@gbio.i3bsh.es